Pergamon

Materials Research Bulletin 37 (2002) 1123–1131

Materials Research Bulletin

High temperature thermoelectric properties of (Ca, Ce)$_4$Mn$_3$O$_{10}$

Yuqin Zhou*, Ichiro Matsubara, Ryoji Funahashi, Gaojie Xu, Masahiro Shikano

National Institute of Advanced Industrial Science and Technology, 1-8-31, Midorigaoka, Ikeda, Osaka 563-8577, Japan

(Refereed)
Received 2 January 2002; accepted 28 February 2002

Abstract

Thermoelectric (TE) properties such as resistivity (ρ), Seebeck coefficient (S), and thermal conductivity (κ) of $Ca_{4-3x}Ce_{3x}Mn_3O_{10}$ ($0 < x \leq 0.03$) polycrystalline samples were measured from room temperature to 1000 K. ρ shows an obvious decrease with the increment of Ce content. The hopping conduction mechanism is used to explain the conduction behavior of these samples. The negative S values indicate that these materials are n-type. The sample of $x = 0.03$ has the largest power factor, 0.52×10^{-4} Wm^{-1} K^{-2} at 1000 K. The value of κ and the dimensionless figure of merit of this sample is 1.51 Wm^{-1} K^{-1} and 0.034 at 1000 K, respectively.

Keywords: A. Oxides; B. Chemical synthesis; C. X-ray diffraction; D. Electric properties; D. Thermal conductivity

1. Introduction

As a power generation system without moving parts and without inducing any pollution, the thermoelectric (TE) generation system has long been studied for several decades and has again attracted interest recently for the ecological environmental needs. The figure of merit, $Z = S^2\sigma/\kappa$, is a primary criterion for evaluating the performance of the TE materials constituting the devices, where S, σ, and κ is the Seebeck coefficient, electrical conductivity, and thermal conductivity, respectively.

* Corresponding author. Tel.: +81-727-51-9541; fax: +81-727-51-9622.
E-mail address: yq-zhou@aist.go.jp (Y. Zhou).

0025-5408/02/$ – see front matter
PII: S0025-5408(02)00730-4

Practical applications generally require $ZT \geq 1$ (T, absolute temperature). TE semiconductors, such as PbTe, Bi_2Te_3, can satisfy the above demand, but they are easily decomposed or oxidized at high temperature in air. Therefore, practical utilization of these materials as a power generator has been limited. With respect to high-temperature operation in air, the advantages of metal oxides are very obvious for their excellent stability to heat. However, the previous guiding principles indicated that the metal oxides are not suitable for TE applications due to their low mobilities. Recently, Terasaki et al. have reported on a new TE oxide material, which breaks the previous guiding principles [1]. In their work, $NaCo_2O_4$ is suggested as a potential p-type TE material with a large thermopower 100 $\mu V\ K^{-1}$ and a low resistivity 0.2 $m\Omega$ cm at 300 K. After that, a series of work on the cobalt oxides have been published [2–11]. Among these works, Funahashi et al. have reported that (Ca, Bi, Sr)–Co–O whiskers have a ZT value over 1.2 at $T > 873$ K in air [4]. This result indicates that the cobalt oxides as p-type TE materials can meet the requirement $ZT \geq 1$ and at the same time have quite good high-temperature stability. Therefore, these materials are potentially useful for TE generator applications.

As another indispensable part of TE conversion device, n-type oxide TE materials have been investigated extensively. Many oxide materials have been studied as n-type candidates, such as In_2O_3-based oxides [12], $(Ca_{0.9}M_{0.1})MnO_3$ (M = Y, La, Ce, Sm, In, Sn, Sb, Pb, Bi) [13,14], $(Zn_{1-x}Al_x)O$ [15–17], Y_2O_3 [18], $Nd_{2-x}Ce_xCuO_4$ [19], $(ZnO)_mIn_2O_3$ [20–22], $Sr_{1-x}La_xPbO_3$ [23], $Ba_{1-x}Sr_xPbO_3$ [24], etc. However, up to date, no n-type oxide material with TE performance comparable to that of the cobalt oxides has been found. Hence, further investigations are still needed to find a potential n-type oxide TE material.

Since Hicks and Dresselhaus have predicted that ZT for a superlattice system should be substantially enhanced relative to the corresponding bulk materials [25,26], considerable attention have been focused on the low-dimensional systems. Recently, Venkatasubramanian et al. have reported superlattice TE thin films that demonstrate a significant enhancement in ZT at 300 K, compared to state-of-the-art bulk Bi_2Te_3 alloys [27]. It, therefore, becomes very interesting to study the TE performance of layered compounds. Recently, Fisher et al. have reported a systematic study on the thermopower of La-doped $Ca_{n+1}Mn_nO_{3n+1}$ ($n = 1, 2,$ and ∞) [28], and claimed that these compounds are n-type materials and their absolute values of thermopower are quite large. However, to our knowledge, no one has reported a systematic TE investigation of these so-called Ruddlesden–Popper (RP) compounds $Ca_{n+1}Mn_nO_{3n+1}$ ($n = 1, 2, 3,$ and ∞), except for Ohtaki et al., who reported a maximum ZT value of 0.16 at 900°C for $CaMn_{0.9}In_{0.1}O_3$ ($n = \infty$) [14]. In this work, we have focused on the $n = 3$ member due to its relatively low ρ, and studied its high temperature TE performance.

2. Experimental

Polycrystalline samples $Ca_{4-3x}Ce_{3x}Mn_3O_{10}$ ($x = 0, 0.01, 0.015, 0.02, 0.03,$ and 0.04) were prepared by solid-state reaction method. After the well-ground stoichiomatric

mixtures of $CaCO_3$, CeO_2, and Mn_2O_3 powders had been prepared, a relatively low-temperature heating sequence were carried out, heated at 800°C for 24 h, 1000°C for 30 h, and 1200°C for 48 h in air with intermediate grindings. And then, the final heating was carried out at 1310°C for 48 h in air for all the samples.

X-ray diffraction (XRD) patterns of the powder samples were obtained on a RIGAKU diffractometer with Cu Kα radiation to examine the sample purities. The high-pure silicon powder was mixed with the sample powder as an internal standard to calibrate the system errors. The samples for electrical measurement were cut out from the sintered pellets as rectangular bars. Two Pt wires were tightly bound around the bars and pasted by Pt conductive paste. Pt/Pt–Rh thermocouples were attached on both end surfaces of the sample by Pt paste. The temperature dependence of ρ was measured using a standard four probe method by taking each Pt leg of thermocouples as current leads and two Pt wires as voltage leads. The thermoelectromotive force (ΔV) and temperature difference (ΔT) of both ends of sample were measured and S was obtained by $\Delta V/\Delta T$. The thermal conductivity κ was determined from the thermal diffusivity and the specific heat capacity, which was measured by the laser flash technique on a RIGAKU thermal constant measurement system. The experiment detail and the laser flash technique were described in [29]. The measurements were carried out for sample disks approximately 10 mm in diameter and 1–2 mm in thickness from room temperature to 1000 K in vacuo. The bulk density of the sintered sample was measured by Archimedes' method.

3. Results and discussions

Fig. 1 shows the XRD patterns of $Ca_{4-3x}Ce_{3x}Mn_3O_{10}$ ($x = 0$, 0.01, 0.015, 0.02, 0.03, and 0.04). Except for the sample of $x = 0.04$ with a small amount of impurity

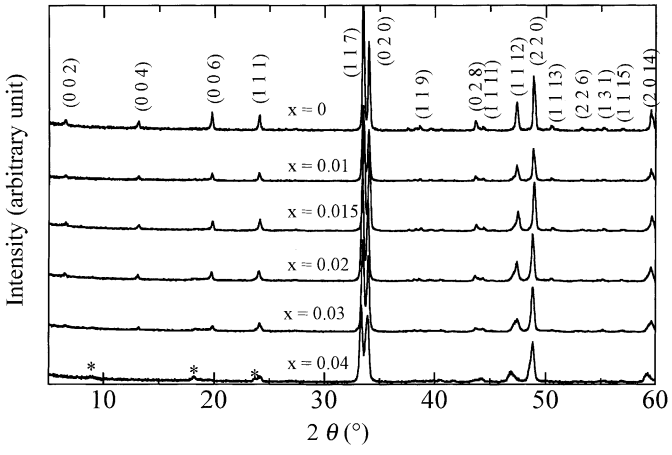

Fig. 1. XRD patterns of $Ca_{4-3x}Ce_{3x}Mn_3O_{10}$ ($x = 0$, 0.01, 0.015, 0.02, 0.03, and 0.04). Impurity phase is pointed out by the asterisk.

Table 1
Bulk density, relative density, electrical resistivity at room temperature (ρ_{RT}), lattice parameter, and cell volume for $Ca_{4-3x}Ce_{3x}Mn_3O_{10}$ ($x = 0$, 0.01, 0.015, 0.02, 0.03)

x value	Bulk density (g cm^{-3})	Relative density (%)	ρ_{RT}	Lattice parameter			Cell volume (Å^3)
				a (Å)	b (Å)	c (Å)	
0	3.326	84	585	5.2646(6)	5.2630(4)	26.8286(4)	743.42(3)
0.01	2.891	69	86	5.2641(7)	5.2630(5)	26.8294(5)	743.28(2)
0.015	2.785	65	62	5.2620(10)	5.2659(7)	26.8112(7)	742.9(2)
0.02	2.682	63	50	5.2620(8)	5.2672(6)	26.8096(5)	743.03(7)
0.03	2.843	65	40	5.2615(20)	5.2697(15)	26.7918(15)	742.6(2)

marked by asterisks, all the peaks can be indexed as the RP phase with orthorhombic symmetry. The cell parameters were refined from the XRD data by a least-square method, as shown in Table 1. For the undoped sample, we obtained that, $a = 5.2646(6)$ Å, $b = 5.2630(4)$ Å, $c = 26.8286(4)$ Å, consistent with the data ($a = 5.26557(12)$, $b = 5.26039(11)$, $c = 26.8276(5)$ Å) reported by Battle et al. [30]. The $x = 0.01$ sample has almost the same cell parameters as the undoped sample because of the very small amount of Ce content. As expected, substitution of smaller Ce^{4+} ion ($r = 0.87$ Å) for the larger Ca^{2+} ion ($r = 1.00$ Å) [31] results in the decrease of the c length. However, with Ce^{4+} substitution, Mn^{3+} is formed with d^{4+} ($t_{2g}^3 e_g^1$) electronic configuration, and the ionic radius of Mn^{3+} larger than that of Mn^{4+}, could possibly increase the a length or b length. As listed in Table 1, with increasing the Ce substitution, although the a lengths almost do not change within the error range, the b lengths obviously increase and the c lengths decrease. The systematical change in lattice parameters and cell volumes indicates that Ce is indeed doped into the bulk of the samples.

The temperature dependencies of ρ are shown in Fig. 2. Because all the samples were prepared in air, the oxygen stoichiometry is not perfect. Therefore, the resistivity of the undoped sample is reasonable smaller than the reported value by Fawcett et al. [32]. In fact, Mihut et al. [33] reported that the room temperature resistivity of $Ca_4Mn_3O_{10-\delta}$ is about 220 mΩ cm. Their sample was also prepared in air. With increasing the Ce content, the carrier concentration is progressively increased. Consequently, the magnitude of ρ systematically decreases. By comparing with the data reported in [13], ρ of $Ca_{4-3x}Ce_{3x}Mn_3O_{10}$ is obviously higher than that of $Ca_{1-y}Ce_yMnO_3$. This is attributed to the difference in structures of these two systems. It is known that $CaMnO_3$ has the perovskite-type structure characterized by a three-dimensional (3D) array of corner-sharing MnO_6 octahedra. However, in the $Ca_4Mn_3O_{10}$, every three $CaMnO_3$ perovskite layers is separated by a rock-salt layer. Therefore, the larger ρ of $Ca_4Mn_3O_{10}$ is reasonably associated with the introduction of the insulating rock-salt type CaO layers between the perovskite blocks. In addition to such an intrinsic reason, the microstructure of the $Ca_{4-3x}Ce_{3x}Mn_3O_{10}$ sintered body could induce the increment of ρ. The relative densities of $Ca_{4-3x}Ce_{3x}Mn_3O_{10}$ are very low, seen in Table 1, indicating the presence of a lot of pores included in the

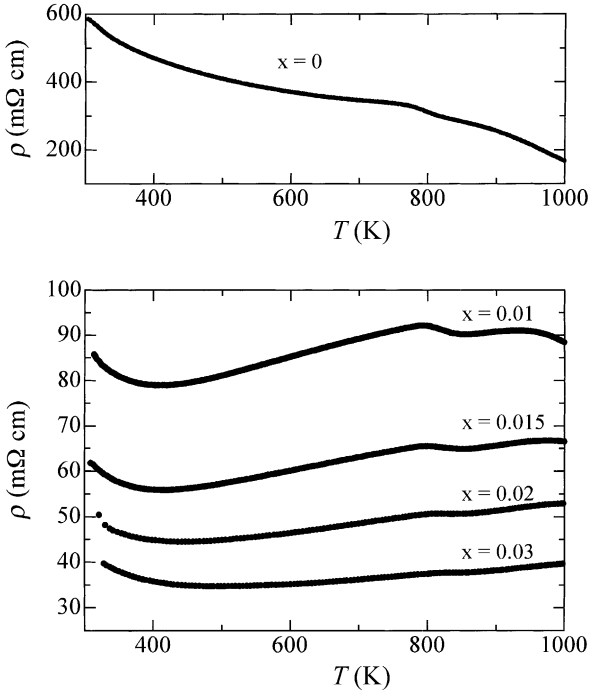

Fig. 2. T dependence of ρ of $Ca_{4-3x}Ce_{3x}Mn_3O_{10}$ ($x = 0$, 0.01, 0.015, 0.02, 0.03).

sintered body. Moreover, as a preferred grain orientation was not obtained, the c-axis component of ρ was picked up in the ρ–T data. The densification and grain orientation could possibly reduce the in-plane ρ value to closer to that of $Ca_{1-y}Ce_yMnO_3$.

In the frame of the polaron hopping conduction mechanism, the following formula is used to fit our data:

$$\sigma = \left(\frac{C}{T}\right)\exp\left(\frac{-E_H}{kT}\right),$$

where C, k, and E_H are a constant, Boltzmann constant and the hopping energy, respectively [34]. This formula predicts a linear relation between $\log \sigma T$ and $1/T$, and $-E_H/k$ is the slope of the straight line. The curves of $\log \sigma T$ versus $1000/T$ of the samples are shown in Fig. 3. A linear fit of the data is consistent in the temperature region $330 < T < 780$ K. Moreover, the samples with higher Ce doping retain linearity in a wider temperature range. In fact, as pointed out by Maignan et al. [35], in the system of $Ca_{1-x}Sm_xMnO_3$, due to the mechanism of carrier creation (non-isovalent cationic substitution) and considering the Jahn–Teller effect (the distortion of MnO_6 octahedra due to $t_{2g}^3 e_g^1$ configuration), a continuous formation of small polarons with increasing doping content is expected.

It is interesting to note that a peak appears around 800 K in the ρ–T curves shown in Fig. 2. It was observed in both the heating and cooling process during the measurements. The anomalies systematically disappear when the Ce content increases.

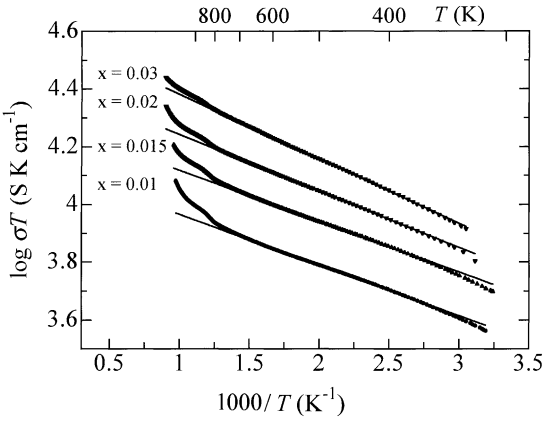

Fig. 3. The relation between log σT and 1000/T.

Therefore, the anomalies are found to be an intrinsic properties of (Ca, Ce)$_4$Mn$_3$O$_{10}$ phase. We did not obtain any evidence of phase transition around 800 K in TG and DTA curves. So it would come from the electric phase transition or spin transition.

Having a large absolute value of S is critical for potential TE materials. The temperature dependences of S of $Ca_{4-3x}Ce_{3x}Mn_3O_{10}$ are shown in Fig. 4. The straight line is fitted by a least-square method. All the S values are negative, indicating that the samples are n-type materials. The absolute values of S of all samples increase with increasing temperature within the whole temperature range measured and decrease with increasing the Ce content. At 1000 K, the absolute values of S of our samples are all larger than 140 $\mu V\ K^{-1}$, showing the advantage for TE application. It is interesting to note that the temperature dependence of S is well fitted by a straight line, $S = S_0 + T(dS/dT)_0$, which is not expected from the principles of hopping mechanism [36]. In fact, such a case has been reported, for example, for $LaCrO_3$ [37], and $(Ca_{0.9}M_{0.1})MnO_3$ (M = Y, La, Ce, Sm, In, Sn, Sb, Pb, Bi) [13].

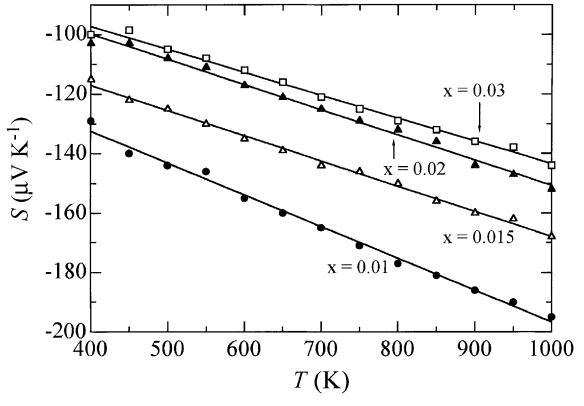

Fig. 4. T dependence of S. The straight line is fitted by the least-square method.

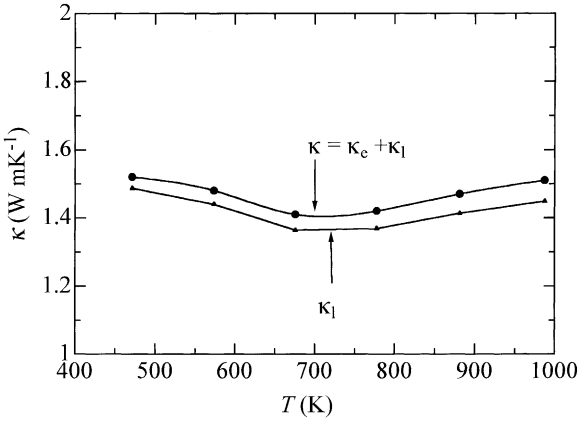

Fig. 5. T dependence of κ and κ_l of $Ca_{3.91}Ce_{0.09}Mn_3O_{10}$. The solid line is a guide for eyes.

From the definition of Z, a low thermal conductivity κ of the material is required to keep the temperature difference large enough. $Ca_{3.91}Ce_{0.09}Mn_3O_{10}$ has the largest power factor, 0.052×10^{-3} Wm^{-1} K^{-2}, among all the samples, and its temperature dependence of κ is shown in Fig. 5. The specific heat and thermal diffusivity at room temperature of this sample is 0.895 J kg^{-1} and 0.00573 cm^2 s^{-1}, respectively. In general, κ can be expressed by the sum of a lattice component (κ_l) and an electronic component (κ_e) as $\kappa = \kappa_l + \kappa_e$. And $\kappa_e = L\sigma T$, where L is the Lorenz number. Here, $L = 2.45 \times 10^{-8}$ W Ω K^{-2} is employed to calculate the κ_e [38]. Hence, κ_l is obtained from $\kappa - \kappa_e$ and is also shown in Fig. 5. It is clear that κ comes largely from the lattice component contribution, so the value of κ is closely related to the crystallographic structure of samples. The κ value of $Ca_{3.91}Ce_{0.09}Mn_3O_{10}$ is 1.52–1.51 W mK^{-1} from 470 to 987 K, less than a half of that of $Ca_{0.9}Bi_{0.1}MnO_3$ reported by [13]. In addition to the difference in the bulk density, a low κ value of $Ca_{3.91}Ce_{0.09}Mn_3O_{10}$ could be

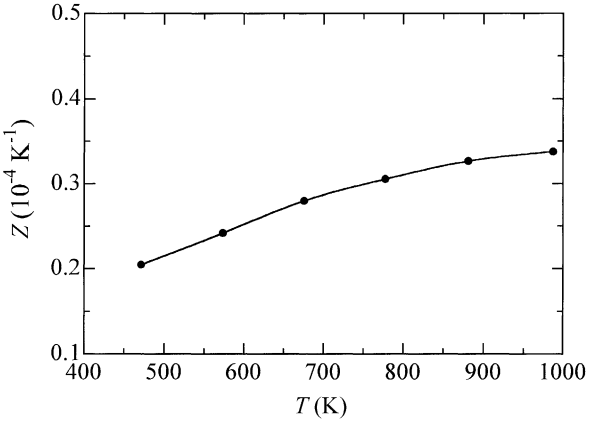

Fig. 6. T dependence of Z of $Ca_{3.91}Ce_{0.09}Mn_3O_{10}$. The solid line is a guide for eyes.

attributed partly to the suppression by phonon scattering at the rock-salt layer between the perovskite blocks.

The temperature dependence of Z of $Ca_{3.91}Ce_{0.09}Mn_3O_{10}$ is shown in Fig. 6. The Z value increases with increasing T, and at 1000 K, $ZT = 0.034$. The improvement of the microstructure could reduce ρ as described above and hence increase ZT. However, TE performance of the layered perovskite manganites does not seem to exceed that of the 3D simple perovskite manganites.

4. Conclusions

TE properties of the $n = 3$ member of the RP compounds, $(Ca, Ce)_4Mn_3O_{10}$, were investigated for the first time in detail from room temperature to 1000 K. The conduction behaviors of these samples were explained by the polaron hopping mechanism. The temperature dependence of S indicated them as n-type materials. κ was separated into a small electron component and a large phonon component by applying the Wiedemann–Franz law. The dimensionless figure of merit ZT of $Ca_{3.91}Ce_{0.09}Mn_3O_{10}$ is 0.034 at 1000 K. A certain improvement of TE performance could be achieved by a reduction of ρ.

Acknowledgments

This work was supported in part by the New Energy and Industrial Technology Development Organization (NEDO) of Japan's Industrial Technology Research Grant Program in 2000.

References

[1] I. Terasaki, Y. Sasago, K. Uchinokura, Phys. Rev. B 56 (1997) R12685.
[2] S. Li, R. Funahashi, I. Matsubara, K. Ueno, H. Yamada, J. Mater. Chem. 9 (1999) 1659.
[3] R. Funahashi, I. Mastubara, S. Sodeoka, Appl. Phys. Lett. 76 (17) (2000) 2385.
[4] R. Funahashi, I. Matsubara, H. Ikuta, T. Takechi, U. Mizutani, S. Sodeoka, Jpn. J. Appl. Phys. 39 (2000) L1127.
[5] S. Li, R. Funahashi, I. Mastubara, K. Ueno, H. Yamada, Chem. Mater. 12 (2000) 2424.
[6] Y. Miyazaki, K. Kudo, M. Akoshima, Y. Ono, Y. Koike, T. Kajitani, Jpn. J. Appl. Phys. 39 (2000) L531.
[7] T. Itoh, I. Terasaki, Jpn. J. Appl. Phys. 39 (2000) 6658.
[8] W. Shin, N. Murayama, J. Mater. Res. 15 (2000) 382.
[9] R. Funahashi, I. Mastubara, Appl. Phys. Lett. 79 (2001) 362.
[10] I. Mastubara, R. Funahashi, T. Takeuchi, S. Sodeoka, J. Appl. Phys. 90 (2001) 462.
[11] I. Mastubara, R. Funahashi, T. Takeuchi, S. Sodeoka, T. Shimizu, K. Ueno, Appl. Phys. Lett. 78 (2001) 3627.
[12] M. Ohtaki, D. Ogura, K. Eguchi, H. Arai, J. Mater. Chem. 4 (1994) 653.
[13] M. Ohtaki, H. Koga, T. Tokunaga, K. Eguchi, H. Arai, J. Solid State Chem. 120 (1995) 105.
[14] M. Ohtaki, T. Tokunaga, K. Eguchi, H. Arai, in: Proceedings of the 16th International Conference on Thermoelectrics, 1997, p. 224.

[15] M. Ohtaki, T. Tsubota, K. Eguchi, H. Arai, J. Appl. Phys. 79 (1996) 1816.
[16] T. Tsubota, M. Ohtaki, K. Eguchi, H. Arai, J. Mater. Chem. 7 (1) (1997) 85.
[17] T. Tsubota, M. Ohtaki, K. Eguchi, H. Arai, J. Mater. Chem. 8 (2) (1998) 409.
[18] K. Koumoto, W.S. Seo, S. Ozawa, Appl. Phys. Lett. 71 (1997) 1475.
[19] M. Yasukawa, N. Murayama, J. Mater. Sci. 32 (1997) 6489.
[20] H. Ohta, W.S. Seo, K. Koumoto, J. Am. Ceram. Soc. 79 (8) (1996) 2193.
[21] M. Kazeoka, H. Hiramatsu, W.S. Seo, K. Koumoto, J. Mater. Res. 13 (1998) 523.
[22] Y. Masuda, M. Ohta, W.W. Seo, W. Pitschke, K. Koumoto, J. Solid State Chem. 150 (2000) 221.
[23] I. Terasaki, T. Nonaka, J. Phys.: Condens. Matter 11 (1999) 5577.
[24] M. Yasukawa, N. Murayama, J. Mater. Sci. Lett. 16 (1997) 1731.
[25] L.D. Hicks, M.S. Dresslhaus, Phys. Rev. B 47 (1993) 12727.
[26] L.D. Hicks, M.S. Dresslhaus, Phys. Rev. B 47 (1993) 16631.
[27] R. Venkatasubramanian, E. Siivola, T. Colpitts, B. O'Quinn, Nature 413 (2001) 597.
[28] B. Fisher, L. Patlagan, G.M. Reisner, A. Knizhnil, Phys. Rev. B 61 (2000) 470.
[29] W.J. Parker, R.J. Jenkins, C.P. Butler, G.L. Abbott, J. Appl. Phys. 32 (1961) 1679.
[30] P.D. Battle, M.A. Green, J. Lago, J.E. Millburn, M.J. Rosseinsky, J.F. Vente, Chem. Mater. 10 (1998) 658.
[31] R.D. Shannon, Acta Crystallogr. A 32 (1976) 751.
[32] I.D. Fawcett, J.E. Sunstrom IV, M. Greenblatt, M. Croft, K.V. Ramanujachary, Chem. Mater. 10 (1998) 3643.
[33] A.I. Mihut, L.E. Spring, R.I. Bewley, S.J. Blundell, W. Hayest, T. Jestadt, B.W. Lovett, R. Mcdonald, F.L. Pratt, J. Singleton, P.D. Battle, J. Lago, M.J. Rosseinsky, J.F. Vente, J. Phys.: Condens. Matter 10 (1998) L727.
[34] D.P. Karim, A.T. Aldred, Phys. Rev. B 20 (1979) 2255.
[35] A. Maignan, C. Martin, F. Damay, B. Raveau, J. Hejtmanek, Phys. Rev. B 58 (1998) 2758.
[36] H.L. Tuller, A.S. Nowick, J. Phys. Chem. Solids 38 (1977) 859.
[37] W.J. Weber, C.W. Griffin, J.L. Bates, J. Am. Ceram. Soc. 70 (1987) 265.
[38] M.E. Fine, N. Hsieh, J. Am. Ceram. Soc. 57 (1974) 502.